IEEE Access
Multidisciplinary | Rapid Review | Open Access Journal

Received March 22, 2020, accepted April 20, 2020, date of publication April 24, 2020, date of current version May 15, 2020.

Digital Object Identifier 10.1109/ACCESS.2020.2990290

Low Refractive-Index and Temperature Sensitive Torsion Sensor Based on Cascaded Long-Period Fiber Gratings Inscribed in a Four-Mode Fiber

JIE DONG, MEI SANG, SHUANG WANG, TIANHUA XU, LEI YANG, XUN YU, AND TIEGEN LIU

School of Precision Instrument and Opto-Electronics Engineering, Tianjin University, Tianjin 300072, China
Key Laboratory of Opto-Electronics Information Technology, Tianjin University, Ministry of Education, Tianjin 300072, China

Corresponding authors: Mei Sang (m_sang@tju.edu.cn) and Shuang Wang (sarahwang@tju.edu.cn)

This work was supported in part by the National Key Research and Development Project of China under Grant 2018YFF01013203, in part by the Science Foundation Project of Tianjin City under Grant14RCGFGX00844, and in part by the Seed Foundation of Tianjin University under Grant 2020XYF-0045.

ABSTRACT Torsion sensing is a promising technique in a variety of different scientific and industrial applications. In this paper, we present a novel torsion sensor based on the cascaded long-period fiber grating inscribed in a four-mode fiber (CLPFG-FMF). The change in rotatory vector makes resonant wavelength shift, for the twisted CLPFG-FMF. The key factor, which severely impacts on the properties and performance of torsion sensor, is also investigated and discussed. Experimental results show that the resonant wavelength linearly shifts with the torsion rate and the cascaded angle plays an important role in enhancing torsion sensitivity. The proposed torsion sensor achieves optimal sensitivities of -0.519 nm/(rad/m) in counterclockwise and 0.501 nm/(rad/m) in clockwise. The repeatability and stability of the CLPFG-FMF with cascaded angle of 0° are studied as well. The refractive index sensitivity of the CLPFG-FMF with cascaded angle of 0° is −5.20 nm/RIU from 1.3431 to 1.4374 refractive index ranges and the temperature sensitivity is −0.0173 nm/°C from 25 °C to 90 °C. The high sensitivity of torsion sensing is expected to be useful for broad applications across engineering fields.

INDEX TERMS Angularly cascaded, four-mode fiber, long-period fiber grating, torsion sensor.

I. INTRODUCTION

The ability to quantify the deformation by measuring the magnitude of torsion is instrumental in evaluating structural integrity and it is essential for the security monitoring of civil engineering, including bridges, buildings, dams, and other structures [1]. Compared to conventional electronic techniques, torsion sensors based on optical fiber have the excellent merits of high sensitivity, compact size, easy fabrication, and immunity to electromagnetic interference [2]. These advantages have attracted considerable attention in related fields. To date, various sorts of fiber-optic torsion sensors have been implemented and reported, including Mach-Zehnder interferometers [3], bi-core fibers [4], hollow-core fibers [5], twin-core fibers [6], fiber Bragg gratings (FBGs) [7], and long-period fiber gratings (LPFGs) [8]. Wherein, the LPFG can achieve a high sensitivity by measuring the change in the rotatory vector caused by the twist-induced birefringence [9]. There are a lot of methods for fabricating LPFG, such as ultraviolet laser radiation [10], electric arc [11], and mechanical deformation [12]. However, most of these sensors cannot distinguish the direction of torsion, which makes them invalid in some applications.

In order to address this issue, a promising method of fabricating the LPFG by a high-frequency CO_2 laser pulse has been proposed. Due to the unilateral exposure to the CO_2 laser, the LPFG has the capability of torsion dependence and it can distinguish the direction of torsion. Today, there are a great deal of torsion sensors based on the LPFG fabricated by a high-frequency CO_2 laser pulse, such as double cladding fiber chiral LPFG [13], helical LPFG [14], cascaded LPFG [15], and segmented LPFG [16]. The coupling of light from the core mode into co-propagating cladding modes in LPFGs results in acute sensitivity of the cladding mode effective refractive index to the environment. Thus, the torsion sensitivity is affected by other factors, including refractive index and temperature. To overcome the intrinsic limitation, the LPFG inscribed in a four-mode fiber (LPFG-FMF)

The associate editor coordinating the review of this manuscript and approving it for publication was Muguang Wang.

has been proposed and demonstrated. Since the LPFG-FMF originates from coupling between the two core modes, it is insensitive to the changes in the refractive index and temperature [17], [18].

In this paper, we present a torsion sensor based on the cascaded LPFG-FMF (CLPFG-FMF) fabricated by a high-frequency CO_2 laser pulse, for the first time to our knowledge. The sensor consists of two identical LPFG-FMFs with cascaded angle of 0°. Because of the elliptical birefringence, the transmission spectrum changes with the torsion rate. The cascaded angle of two LPFG-FMFs has benefits of enhancing sensitivity. By comparing the torsion sensitivities of CLPFG-FMFs with different cascaded angles, 0° is corresponding to the highest sensitivity of −0.519 nm/(rad/m) in counterclockwise and 0.501 nm/(rad/m) in clockwise, respectively. The repeatability and stability are verified experimentally. In addition, the proposed sensor has low refractive index and temperature sensitivities.

II. PRINCIPLE

According to the phase-matching condition, the resonant wavelength of the LPFG-FMF originated from coupling between the LP_{01} and LP_{11} core modes is calculated

$$\lambda_{res} = (n_{eff,01} - n_{eff,11}) \cdot \Lambda, \tag{1}$$

where, λ_{res} represents the resonant wavelength, $n_{eff,01}$ and $n_{eff,11}$ stand for the effective refractive index of the LP_{01} and LP_{11} core modes, respectively. Λ is the LPFG-FMF period. Because the refractive index modulation plane of each period in cross-section is parallel to each other along the fiber axis, the period of the LPFG-FMF is barely affected by the torsion. Hence, the variation in $n_{eff,01}$-$n_{eff,11}$ is a dominated factor affecting the torsion sensitivity. When the torsion is applied on the LPFG-FMF, the wavelength shift is deduced from (1)

$$\Delta\lambda_{res} = (\delta n_{eff,01} - \delta n_{eff,11}) \cdot \Lambda, \tag{2}$$

here, $\delta n_{eff,01}$ and $\delta n_{eff,11}$ denote the changes in the effective refractive index of the LP_{01} and LP_{11} core modes, and they are dependent on the torsion.

To ensure ease of analysis, the torsion applied on the LPFG is the same in principle, unless stated otherwise. Since the $n_{eff,01}$-$n_{eff,11}$ is smaller than $n_{eff,core}$-$n_{eff,cladding}$, according to the (1), the LPFG-FMF has a larger Λ under the same resonant wavelength, compared to the LPFG inscribed in a single-mode fiber (LPFG-SMF). Hence, the LPFG-FMF with a larger Λ has the higher torsion sensitivity.

The refractive index of the conventional LPFG-FMF is expressed as

$$n(z) = n_0 + \left(\Delta n_1/2\right) cos\left(2\pi z/\Lambda_0 + \phi_g\right), \tag{3}$$

where, z is the position along the LPFG-FMF, n_0 is the effective refractive index of the core mode, Δn_1 is the maximum refractive index modulation, Λ_0 is the central pitch, and Φ_g is the phase of the LPFG-FMF. Thus, the change in phase affects the refractive index, which results in different sensitivities.

Owing to the absorption of fiber, an asymmetric refractive index distribution in the cross-section of the LPFG-FMF is caused by a high-frequency CO_2 laser pulse. This asymmetry gives rise to a linear birefringence, and the direction of the linear birefringence depends strongly on the direction of incidence of CO_2 laser.

For a twisted LPFG-FMF with a linear birefringence, the elliptical birefringence appears. The direction of the elliptical birefringence is given by

$$cos\theta = \frac{|\boldsymbol{\alpha}|\, cos\theta_\alpha}{A} + \frac{|\boldsymbol{\beta}|\, cos\theta_\beta}{A}, \tag{4}$$

here, $\boldsymbol{\beta}$ and $\boldsymbol{\alpha}$ represent the linear birefringence vector and the circular birefringence vector, respectively. θ_β and θ_α represent the directions of the linear birefringence vector and circular birefringence vector, respectively. A is defined as

$$A = \sqrt{|\boldsymbol{\alpha}|^2 + |\boldsymbol{\beta}|^2 + 2\,|\boldsymbol{\alpha}|\,|\boldsymbol{\beta}|\, cos\left(\theta_\alpha - \theta_\beta\right)}. \tag{5}$$

The variation in the refractive index of a twisted LPFG-FMF is derived from (3), and described as

$$\begin{aligned}\Delta n(z) &= \left(\Delta n_1/2\right) cos\left\{2\pi z/\Lambda_0 + \theta\right\} \\ &= (\Delta n_1/2)\left[cos\left(2\pi z/\Lambda_0\right) cos\theta - sin\left(2\pi z/\Lambda_0\right) sin\theta\right].\end{aligned} \tag{6}$$

On the basis of (4) and (6), it can be seen that as the θ_β increases from 0° to π, the $cos\theta$ decreases, and then $\Delta n(z)$ decreases.

The change in the refractive index of a twisted CLPFG-FMF satisfies

$$\Delta n_{CLPFG-FMF}(z) = \Delta n_{LPFG-FMF1}(z) + \Delta n_{LPFG-FMF2}(z). \tag{7}$$

When the $|\boldsymbol{\beta}|$ of each LPFG-FMF is the same, the $\boldsymbol{\Delta} n_{CLPFG-FMF}(z)$ just depends on the $\boldsymbol{\Delta} n_{LPFG-FMF2}(z)$, for the CLPFG-FMFs with different cascaded angles. Assuming the direction of the $\boldsymbol{\beta}_{LPFG-FMF1}$ is parallel to the x-axis, the cascaded angle of the CLPFG-FMF is equivalent to the direction of the $\boldsymbol{\beta}_{LPFG-FMF2}$. Referring to (2) and (6), the torsion sensitivity of the CLPFG-FMF decreases as the cascaded angle increases.

The superposition or cancellation of the rotatory vector causes the resonant wavelength to increase or decrease, respectively. The strengthening or weakening in rotation path makes the resonant wavelength shift towards the longer wavelength or the opposite direction, which is called 'red-shift' or 'blue-shift' in the resonant wavelength.

Additionally, the wavelength shift affected by the refractive index, temperature, and torsion is expressed as

$$\Delta\lambda = K_n \Delta n + K_T \Delta T + K_\tau \Delta\tau, \tag{8}$$

here, K_n, K_T, and K_τ are the absolute values of the refractive index sensitivity, temperature sensitivity, and torsion sensitivity, respectively. Δn, ΔT and $\Delta\tau$ are the changes in the refractive index, temperature, and torsion, respectively.

As long as the initial values of refractive index, temperature, and torsion are specified, the absolute value of torsion sensitivity, which is barely affected by refractive index and temperature, can be obtained.

III. EXPERIMENTS AND DISCUSSIONS

A. FABRICATION OF THE CLPFG-FMFs

The four-mode fiber (core diameter of 16 μm and cladding diameter of 125 μm) used in the experiment, supports four modes in the core (LP_{01}, LP_{02}, LP_{11}, and LP_{12}). The refractive index of its core and cladding are 1.453791 and 1.444, respectively. Fig.1 shows the refractive index distribution of the cross-section.

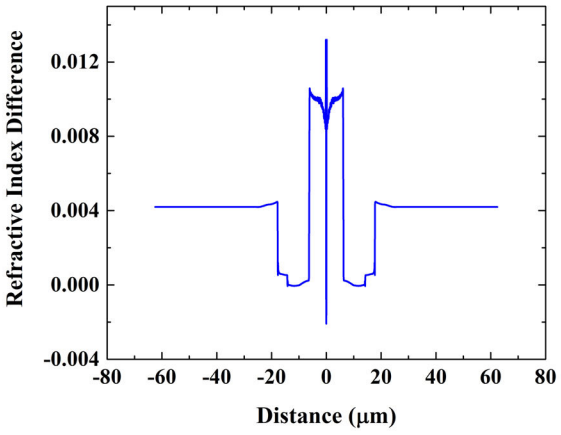

FIGURE 1. Refractive index distribution of the four-mode fiber cross-section.

The phase-matching curve of the LPFG-FMF relying on the coupling between the core modes is depicted in Fig. 2. Taking into account the range of the broadband source (1250–1650 nm), the CLPFG-FMFs relying on coupling between the LP_{01} and LP_{11} core modes with the period of 550 μm and the resonant wavelength of 1500 nm were fabricated.

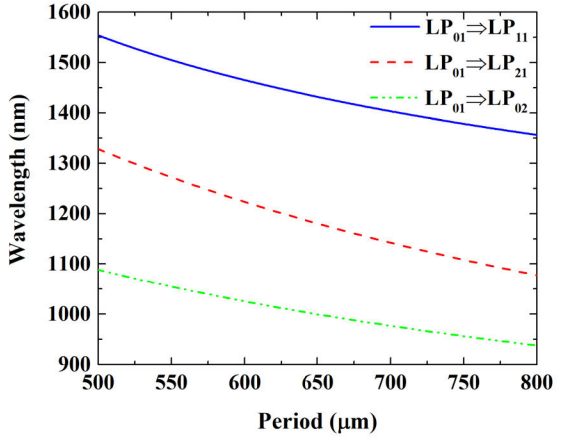

FIGURE 2. Phase-matching curve of the LPFG-FMF relying on the coupling between the core modes.

The fabricating process of the CLPFG-FMF with cascaded angle of 0° is divided into three steps: firstly, the four-mode fiber (length of ∼15 cm) was fixed by two holders, and then the LPFG-FMF with the period of 550 μm and the length of 1.65 cm was fabricated by a high-frequency CO_2 laser pulse with an output power of 10 W and Q frequency of 5 kHz. Secondly, the two holders were moved to the right with the distance of 2.2 cm simultaneously. Finally, the same LPFG-FMF as the previous one was fabricated.

In order to study the impact of the cascaded angle on the sensing performance, the CLPFG-FMFs with cascaded angles of 90° and 180° were fabricated. Except for the second step of fabricating process, in which the two holders were rotated 90° or 180° in clockwise at the same time, the remaining steps were identical to that previously described for the CLPFG-FMF with cascaded angle of 0°. Fig.3 and Fig.4 describe the schematic diagrams and transmission spectra of three CLPFG-FMFs with different cascaded angles, respectively.

B. THE EXPERIMENTAL RESULTS AND DISCUSSIONS

Fig. 5 depicts the schematic diagram of the torsion measurement setup. The broadband source was used and the transmission spectrum was monitored in real-time by an optical spectrum analyzer (MS9740A) with a resolution of 0.03 nm. To keep straight, the CLPFG-FMF was fixed by the two holders. And one holder remained fixed and the other was rotated in clockwise or counterclockwise. The torsion rate is given by

$$\tau = \frac{\theta}{L}, \tag{9}$$

here, θ denotes the rotatory angle of the holder and L refers to the distance between the two holders. In the experiment, L is 20 cm.

The wavelength shifts of three CLPFG-FMFs in torsion rate ranging from −31.32 rad/m to 31.32 rad/m (counterclockwise (−) and clockwise (+) direction) are presented in Fig. 6. With the increasing of torsion rate, the blue-shift and red-shift in the resonant wavelength occur in counterclockwise and clockwise respectively, and the resonant wavelength shifts linearly. Furthermore, the circular birefringence caused by torsion modifies the polarization states. The variation in polarization state impacts on the coupling coefficients of the two modes [19], which results in a decrease in the resonant dip. Simultaneously, the change in polarization states manifests as a resonant wavelength separation. Hence, the transmission spectrum widens as the torsion rate increases [20].

The cascaded angle has a significant effect on torsion sensitivity. Compared to the others, the CLPFG-FMF with cascaded angle of 0° has the highest torsion sensitivity, corresponding to sensitivities of −0.519 nm/(rad/m) and 0.501 nm/(rad/m) in counterclockwise and clockwise, respectively. And the CLPFG-FMF with cascaded angle of 180° has the minimum sensitivities of −0.262 nm/(rad/m) in counterclockwise and 0.289 nm/(rad/m) in clockwise. With the increasing of the cascaded angle, the torsion sensitivities

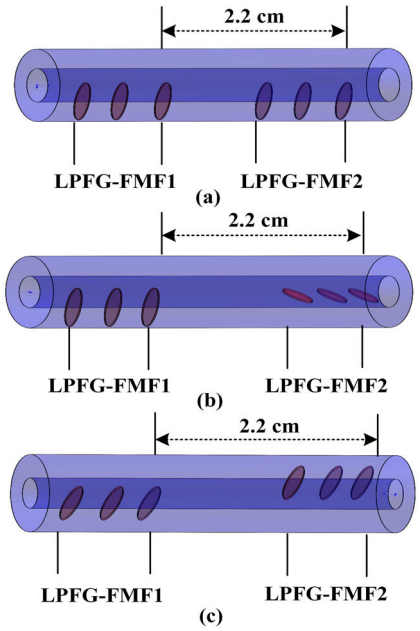

FIGURE 3. Schematic diagrams of the CLPFG-FMFs with cascaded angles of (a) 0°, (b) 90°, and (c) 180°.

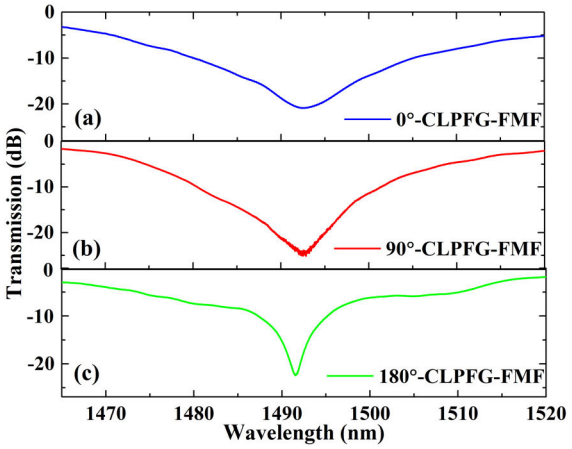

FIGURE 4. Transmission spectra of the CLPFG-FMFs with cascaded angles of (a) 0°, (b) 90°, and (c) 180°, which are measured in air.

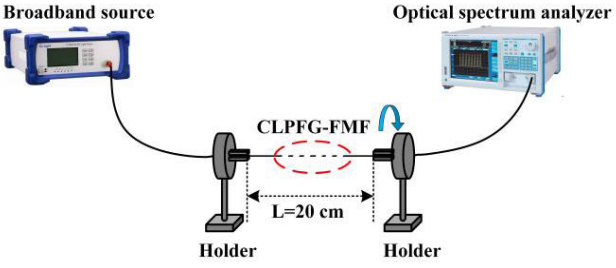

FIGURE 5. Schematic diagram of the torsion measurement setup.

decrease. This tendency is complete agreement with the theoretical analysis in principle.

In order to assess the repeatability, there are three independent measurements from the same CLPFG-FMF with cascaded angle of 0°, and the averages and standard

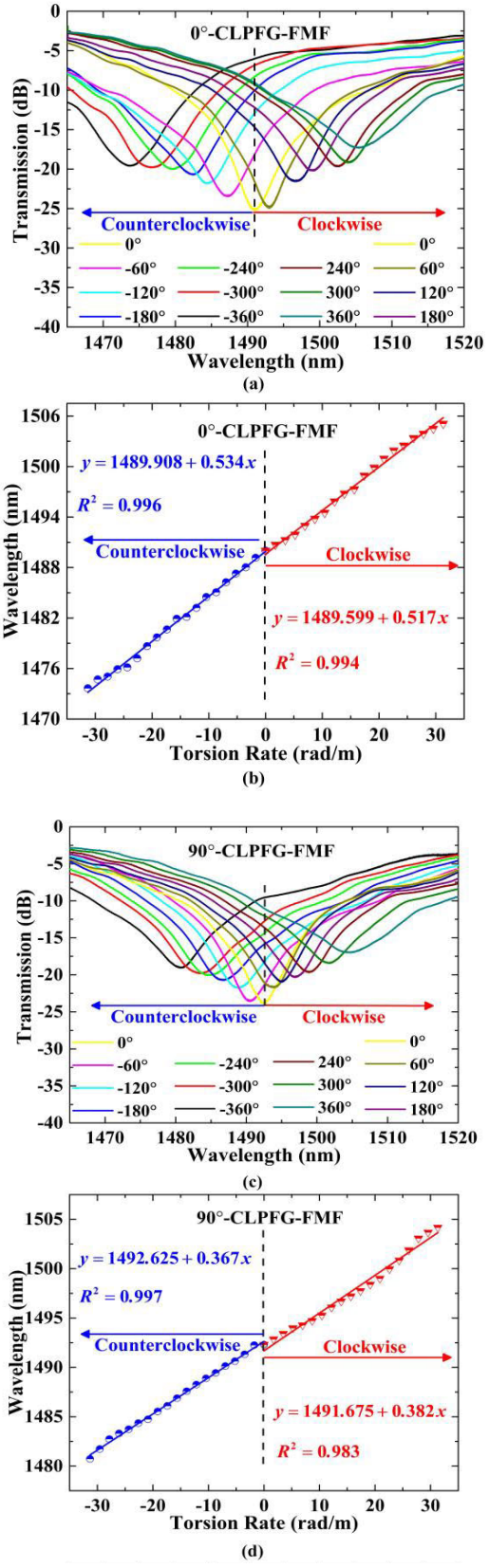

FIGURE 6. Changes in (a) transmission spectrum of CLPFG-FMF with cascaded angle of 0°, (b) wavelength shift of CLPFG-FMF with cascaded angle of 0°, (c) transmission spectrum of CLPFG-FMF with cascaded angle of 90°, (d) wavelength shift of CLPFG-FMF with cascaded angle of 90°.

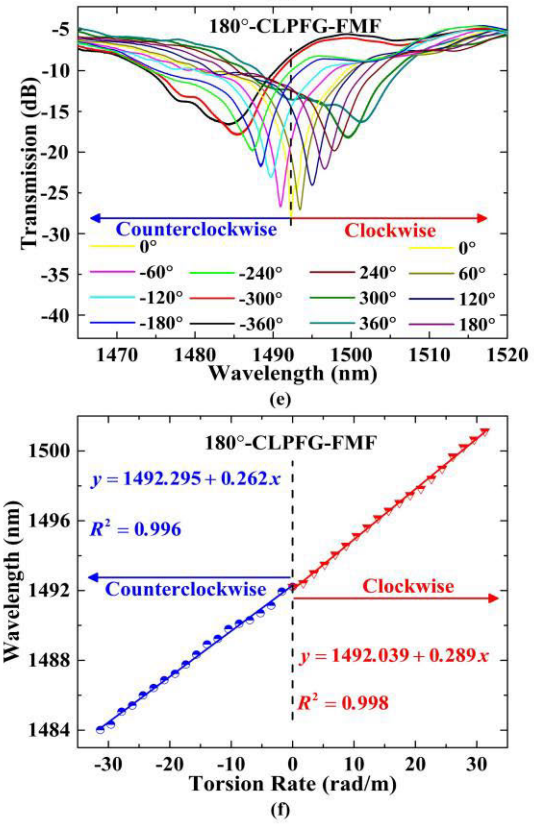

FIGURE 6. *(Continued.)* **Changes in (e) transmission spectrum of CLPFG-FMF with cascaded angle of 180°, (f) wavelength shift of CLPFG-FMF with cascaded angle of 180°, which are measured in torsion rate ranging from −31.32 rad/m to 31.32 rad/m.**

deviations of wavelengths are calculated, as shown in Fig. 7. There are a few differences in the wavelength shifts, which is caused by the variation in stress applied on the CLPFG-FMF. Moreover, the resolution of the optical spectrum analyzer affects the wavelength shift. The experimental result shows that the CLPFG-FMF with cascaded angle of 0° has a good repeatability.

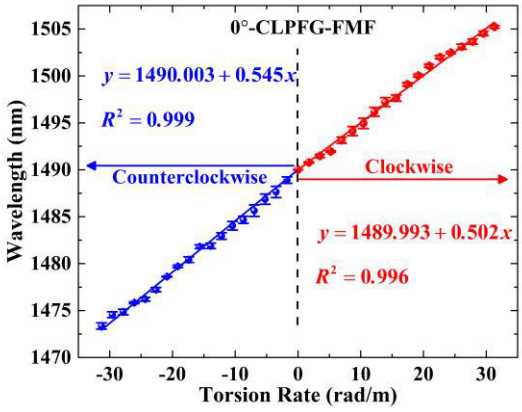

FIGURE 7. **For the CLPFG-FMF with cascaded angle of 0°, the averages and standard deviations of wavelengths in counterclockwise and clockwise.**

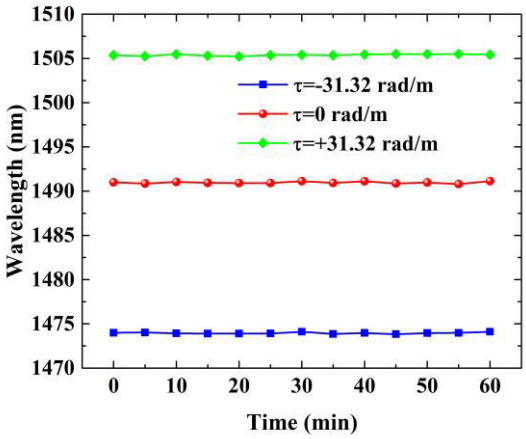

FIGURE 8. **For the CLPFG-FMF with cascaded angle of 0°, the wavelength in the stability measurement, when the torsion rates are −31.32 rad/m, 0 rad/m, and 31.32 rad/m, respectively.**

Fig. 8 describes the resonant wavelength of the CLPFG-FMF with cascaded angle of 0° in the stability measurement. Due to the fluctuation of the laser source, the wavelength fluctuates slightly. When the torsion rates are −31.32 rad/m, 0 rad/m, and 31.32 rad/m, the standard deviations of the measurements are 0.084 nm, 0.109 nm, and 0.090 nm, respectively.

In actual applications, the refractive index and temperature are non-negligible factors affecting the wavelength shift. Hence, the refractive index sensitivity and temperature sensitivity of the CLPFG-FMF with cascaded angle of 0° are investigated experimentally. By putting it into a series of sucrose solutions at a temperature of 25 °C, the resonant wavelength shifts are shown in Fig. 9. The average refractive index sensitivity is −5.20 nm/RIU in the 1.3431–1.4374 refractive index range and the maximum refractive index sensitivity of −14.46 nm/RIU in the refractive index range between 1.4252 and 1.4374 is achieved. The low refractive index sensitivity could be induced by the impurity of the core mode couplings so that mode coupling to small amount of high-order cladding modes may be induced in the four-mode fiber.

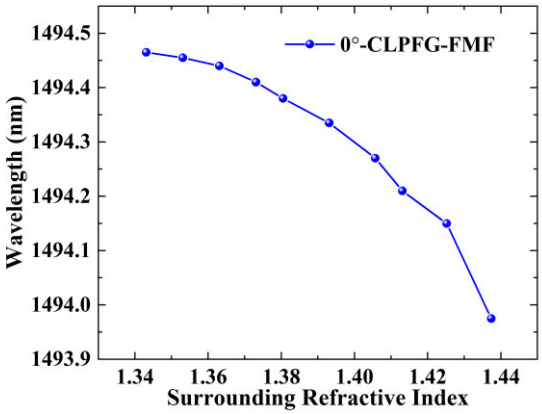

FIGURE 9. **Wavelength shifts of the CLPFG-FMF with cascaded angle of 0°, by putting it into a series of sucrose solutions at a temperature of 25 °C.**

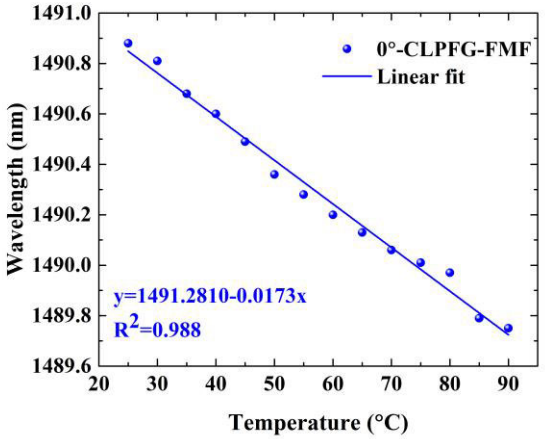

FIGURE 10. Wavelength shifts of the CLPFG-FMF with cascaded angle of 0°, as the temperature increases from 25 °C to 90 °C.

Fig. 10 exhibits the wavelength shifts of the CLPFG-FMF with cascaded angle of 0° in response to the temperature from 25 °C to 90 °C with a step of 5 °C. A blue-shift in the resonant wavelength occurs and the temperature sensitivity is −0.0173 nm/°C. The cross-sensitivities from temperature are 0.0333 (rad/nm)/°C in counterclockwise and −0.0345 (rad/nm)/°C in clockwise.

According to the experimental results, the CLPFG-FMF with cascaded angle of 0° has the low refractive index sensitivity of −5.20 nm/RIU and temperature sensitivity of −0.0173 nm/°C. Based on the measured result, the absolute value of torsion sensitivity is deduced from (8) and described as

$$K_\tau = \frac{\Delta\lambda - (-5.20\text{nm/RIU})\,\Delta n - (-0.0173\text{nm/°C})\,\Delta T}{\Delta\tau}. \tag{10}$$

Considering the resolution of the optical spectrum analyzer (0.03 nm), the torsion resolutions of the sensor are -5.57×10^{-2} rad/m in counterclockwise and 6.48×10^{-2} rad/m in clockwise.

TABLE 1. Comparison of torsion sensitivities between the related schemes and the proposed sensor.

Type	Sensitivity (nm/(rad/m))	Range (rad/m)	Reference
A pair of helical LPFG	0.115	(-5π/2,5π/2)	[21]
A segmented LPFG	0.3 clockwise -0.14 counterclockwise	(-10.35,10.35)	[16]
Seven-core fiber	-0.4	(4.758,40.439)	[22]
Cascaded LPFG	0. 3317 clockwise 0. 3103 counterclockwise	(-25,25)	[15]
Helical LPFG-TMF	0.47	(-30,30)	[17]
CLPFG-FMF	0.501 clockwise -0.519 counterclockwise	(-31.32, 31.32)	This paper

The torsion sensitivities of different types of sensors are listed in Table 1. The proposed sensor has a higher torsion sensitivity and wider measurement range, compared with the previously reported counterparts. Furthermore, it possesses the inherent merits of low cost, good stability, low refractive index and temperature sensitivities.

IV. CONCLUSION

In this paper, we propose and experimentally investigate a torsion sensor based on the CLPFG-FMF, mainly consisting of two identical LPFG-FMFs with cascaded angle of 0°. Experimental results show that the sensor is capable of distinguishing the direction of torsion and the resonant wavelength linearly shifts with the torsion rate. Furthermore, the torsion sensitivity depends strongly on the cascaded angle, and the highest torsion sensitivities of −0.519 nm/(rad/m) in counterclockwise and 0.501 nm/(rad/m) in clockwise are achieved, for the CLPFG-FMF with cascaded angle of 0°. The repeatability and stability of the CLPFG-FMF with cascaded angle of 0° are studied. The refractive index sensitivity is −5.20 nm/RIU in the refractive index ranging from 1.3431 to 1.4374, and the temperature sensitivity is −0.0173 nm/°C from 25 °C to 90 °C, which is one third of that of the conventional LPFGs. Moving forward, the proposed torsion sensor is ideal for measuring torsion and it features a high sensitivity, easy fabrication, low cost, good repeatability and stability, low refractive index and temperature sensitivities, compared with existing conventional LPFGs. It is expected to open new and exciting fields in engineering, including bridges, buildings, dams, and so on.

REFERENCES

[1] L. Shi, T. Zhu, Y.-E. Fan, K. S. Chiang, and Y. Rao, "Torsion sensing with a fiber ring laser incorporating a pair of rotary long-period fiber gratings," *Opt. Commun.*, vol. 284, no. 22, pp. 5299–5302, Oct. 2011, doi: 10.1016/j.optcom.2011.07.049.

[2] B. Song, H. Zhang, Y. Miao, W. Lin, J. Wu, H. Liu, D. Yan, and B. Liu, "Highly sensitive twist sensor employing sagnac interferometer based on PM-elliptical core fibers," *Opt. Express*, vol. 23, no. 12, p. 15372, Jun. 2015, doi: 10.1364/OE.23.015372.

[3] S. Duan, X. Bai, X. Kang, H. Du, W. Liu, T. Geng, C. Tong, C. Sun, X. Jin, C. Lu, Y. Li, W. Sun, and L. Yuan, "High sensitive torsion sensor based on cascaded pre-twisted taper and multi-mode fiber sheets," *IEEE Photon. Technol. Lett.*, vol. 31, no. 19, pp. 1588–1591, Oct. 1, 2019, doi: 10.1109/LPT.2019.2938770.

[4] A. B. L. Ribeiro, S. F. O. Silva, O. Frazão, and J. L. Santos, "Bi-core optical fiber for sensing of temperature, strain and torsion," *Meas. Sci. Technol.*, vol. 30, no. 3, Mar. 2019, Art. no. 035104, doi: 10.1088/1361-6501/ab035b.

[5] D. Liu, R. Kumar, F. Wei, W. Han, A. K. Mallik, J. Yuan, C. Yu, Z. Kang, F. Li, Z. Liu, H.-Y. Tam, G. Farrell, Y. Semenova, and Q. Wu, "Highly sensitive twist sensor based on partially silver coated hollow core fiber structure," *J. Lightw. Technol.*, vol. 36, no. 17, pp. 3672–3677, Sep. 1, 2018, doi: 10.1109/JLT.2018.2842111.

[6] O. Frazão, R. M. Silva, J. Kobelke, and K. Schuster, "Temperature- and strain-independent torsion sensor using a fiber loop mirror based on suspended twin-core fiber," *Opt. Lett.*, vol. 35, no. 16, p. 2777, Aug. 2010, doi: 10.1364/OL.35.002777.

[7] W. Yiping, M. Wang, and X. Huang, "In fiber Bragg grating twist sensor based on analysis of polarization dependent loss," *Opt. Express*, vol. 21, no. 10, May 2013, Art. no. 11913, doi: 10.1364/OE.21.011913.

[8] C. Zhu, S. Ishikami, H. Zhao, and H. Li, "Multichannel long-period fiber grating realized by using the helical sampling approach," *J. Lightw. Technol.*, vol. 37, no. 9, pp. 2008–2013, May 1, 2019, doi: 10.1109/JLT.2019.2897314.

[9] W. Liu, C. Sun, Y. Ma, X. Bai, L. Yu, S. Duan, H. Du, C. Zhao, C. Lu, L. Zhao, T. Geng, and L. Yuan, "A highly sensitive torsion sensor with a new fabrication method," *IEEE Photon. Technol. Lett.*, vol. 31, no. 6, pp. 463–466, Mar. 15, 2019, doi: 10.1109/LPT.2019.2898037.
[10] Y. Wang, X. Huang, and M. Wang, "Temperature insensitive birefringent LPG twist sensing based on the polarization properties," *IEEE Photon. Technol. Lett.*, vol. 27, no. 22, pp. 2367–2370, Nov. 15, 2015, doi: 10.1109/LPT.2015.2466171.
[11] P. Caldas, G. Rego, O. V. Ivanov, and J. L. Santos, "Characterization of the response of a dual resonance of an arc-induced long period grating to various physical parameters," *Appl. Optics.*, vol. 49, no. 16, pp. 2994–2999, Jun. 2010, 10.1364/AO.49.002994.
[12] J. Yong Cho, J. Hoon Lim, and K. Shik Lee, "Optical fiber twist sensor with two orthogonally oriented mechanically induced long-period grating sections," *IEEE Photon. Technol. Lett.*, vol. 17, no. 2, pp. 453–455, Feb. 2005, doi: 10.1109/LPT.2004.840073.
[13] C. Jiang, Y. Liu, L. Huang, and C. Mou, "Double cladding fiber chiral long-period grating-based directional torsion sensor," *IEEE Photon. Technol. Lett.*, vol. 31, no. 18, pp. 1522–1525, Sep. 15, 2019, doi: 10.1109/LPT.2019.2936209.
[14] L. Xian, Y. Wang, D. Wang, and L. Li, "Influence of molten-state duration time on torsion sensitivity for fiber sensors based on helical long-period gratings: An experimental study," *Opt. Fiber Technol.*, vol. 46, pp. 226–229, Dec. 2018, doi: 10.1016/j.yofte.2018.10.016.
[15] L. Wang, W. Zhang, L. Chen, Z. Bai, F. Liu, and T. Yan, "Torsion sensor based on two cascaded long period fiber gratings fabricated by CO2 laser pulse irradiation and HF etching technique respectively," *J. Modern Opt.*, vol. 64, no. 5, pp. 541–545, Mar. 2017, doi: 10.1080/09500340.2016.1249424.
[16] C. Sun, T. Geng, J. He, A. Zhou, W. Yang, X. Jin, X. Chen, Y. Zhou, Q. Hu, and L. Yuan, "High sensitive directional torsion sensor based on a segmented long-period fiber grating," *IEEE Photon. Technol. Lett.*, vol. 29, no. 24, pp. 2179–2182, Dec. 15, 2017, doi: 10.1109/LPT.2017.2768084.
[17] L. Zhang, Y. Liu, Y. Zhao, and T. Wang, "High sensitivity twist sensor based on helical long-period grating written in two-mode fiber," *IEEE Photon. Technol. Lett.*, vol. 28, no. 15, pp. 1629–1632, Aug. 1, 2016, doi: 10.1109/LPT.2016.2555326.
[18] J. L. Dong and K. S. Chiang, "Temperature-insensitive mode converters with CO_2-laser written long period fiber gratings," *IEEE Photon. Technol. Lett.*, vol. 27, no. 9, pp. 1006–1009, May 2015, doi: 10.1109/LPT.2015.2405092.
[19] R. Ulrich and A. Simon, "Polarization optics of twisted single-mode fibers," *Appl. Opt.*, vol. 18, no. 13, pp. 2241–2251, Jul. 1979, doi: 10.1364/AO.18.002241.
[20] Z. H. Zhihang Han, C. S. Cuiting Sun, X. J. Xiren Jin, H. J. Hang Jiang, C. Y. Chong Yao, S. Z. Shuo Zhang, W. L. Weiliang Liu, T. G. Tao Geng, F. P. Feng Peng, W. S. Weimin Sun, and L. Y. Libo Yuan, "A polarization-independent torsion sensor based on the near-helical long period fiber grating," *Chin. Opt. Lett.*, vol. 16, no. 10, 2018, Art. no. 100601, doi: 10.3788/COL201816.100601.
[21] H.-L. Zhang, W.-G. Zhang, L. Chen, Z.-D. Xie, Z. Zhang, T.-Y. Yan, and B. Wang, "Bidirectional torsion sensor based on a pair of helical long-period fiber gratings," *IEEE Photon. Technol. Lett.*, vol. 28, no. 15, pp. 1700–1702, Aug. 1, 2016, doi: 10.1109/LPT.2016.2533478.
[22] C. Liu, Y. Jiang, B. Du, T. Wang, D. Feng, B. Jiang, and D. Yang, "Strain-insensitive twist and temperature sensor based on seven-core fiber," *Sens. Actuators A, Phys.*, vol. 290, pp. 172–176, May 2019, doi: 10.1016/j.sna.2019.03.026.

JIE DONG was born in Shanxi, China, in 1993. She received the B.E. degree from the North University of China, Taiyuan, China, in 2016, and the M.S. degree in optoelectronics from Tianjin University, Tianjin, China, in 2018. Her research interest includes optical fiber sensors.

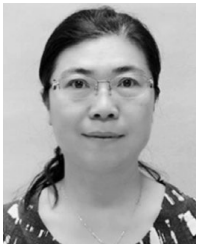

MEI SANG was born in Datong, Shanxi, China, in 1967. She received the M.S. degree in applied physics and the Ph.D. degree in optics from Tianjin University, Tianjin, China, in 1989 and 2004, respectively. From March 2007 to September 2007, she was a National Visiting Scholar, engaged in the research of ultrafast terahertz time domain spectrum measurement with the Department of Electronic and Computer Engineering, Oklahoma State University, USA. Her current research interests include introduction to physical optics and optoelectronics.

SHUANG WANG was born in Tianjin, China, in 1982. She received the M.S. degree from the College of Computer Science and Technology, Shandong University, Shandong, China, in 2005, and the Ph.D. degree in optics from Tianjin University, Tianjin, in 2014. Her research interests include optical fiber sensing technology and photoelectric detection technology and other fields.

TIANHUA XU received the M.S. degree in information engineering from the School of Precision Instrument and Opto-Electronic Engineering, College of Engineering, Tianjin University, in 2005, and the M.E. degree in optical engineering from the School of Precision Instrument and Optoelectronic Engineering, Tianjin University, in 2008, and the Ph.D. degree in microelectronics and applied physics from the Royal Institute of Technology, in 2012. His research interests include optical communication networks, machine learning, digital signal processing, and fiber optic sensor networks.

LEI YANG was a Visiting Scholar with the School of Electronic Information and Engineering, University of Kent, U.K., from March 2017 to September 2017. He was an Associate Professor with Tianjin University, from July 2018 to December 2018. From December 2018 to June 2019, he was a Visiting Scholar with the Department of Electronic Engineering, California Institute of Technology.

XUN YU was born in Shandong, China, in 1993. He received the B.E. degree and M.S. degree in optoelectronics from Tianjin University, Tianjin, China, in 2016 and 2018, respectively. His research interest includes optical fiber sensors.

TIEGEN LIU was born in Tianjin, China, in 1955. He received the B.E., M.E., and Ph.D. degrees in optical engineering from Tianjin University, China, in 1982, 1987, and 1999, respectively. He joined Tianjin University, in 1982, where he is currently a Professor with the College of Precision Instrument and Opto-Electronics Engineering. His research interests include optical fiber sensors, optical polarization technology, and opto-electronics measurement.